PHYSICAL REVIEW B
CONDENSED MATTER

THIRD SERIES, VOLUME 31, NUMBER 3 1 FEBRUARY 1985

Paramagnetic scattering from a cubic ferromagnet Pd_2MnSn

G. Shirane, Y. J. Uemura, and J. P. Wicksted
Physics Department, Brookhaven National Laboratory, Upton, New York 11973

Y. Endoh and Y. Ishikawa
Physics Department, Tohoku University, Sendai 980, Japan

(Received 21 June 1984)

Paramagnetic neutron scattering from the localized, metallic ferromagnet Pd_2MnSn is characterized for the entire range of energy and momentum (ω,Q) space for a temperature range between T_c (193 K) and room temperature. The scattering function $S(Q,\omega)$ can be well described by a simple double Lorentzian form $S(Q,\omega)\propto T[1/(\kappa_1^2+q^2)]\Lambda_1 q^2/[(\Lambda_1 q^2)^2+\omega^2]$ where, for larger q, the q^2 dependence in both Lorentzian factors changes over to a more general functional form. These results are in marked contrast to the case of the cubic, insulating ferromagnet EuO. This study reinforces our current interpretation of the constant-energy ridges which have also been observed in Ni.

I. INTRODUCTION

Despite extensive experimental and theoretical studies[1] in recent years, the ferromagnetism in $3d$ metals has remained one of the least-understood topics of condensed-matter physics. The most interesting ferromagnetics are, of course, Fe and Ni. We have addressed the basic questions concerning the paramagnetic scattering from these ferromagnets in our recent series of neutron scattering studies.[2–5] We have presented a different interpretation from the picture of "persistent spin waves" above T_c, previously advocated by Lynn and Mook[6,7] for Fe and Ni. The main conclusion of our study is that the scattering function $S(Q,\omega)$ follows a simple universal form for a surprisingly wide range of Q, ω, and temperature. We have also conjectured[3,5] that this universal scattering function may be valid for all cubic ferromagnets, including EuO, MnSi, and Pd_2MnSn. The characteristic signature of a particular ferromagnet, such as Ni, may appear via deviations from this universality. However, because of the extremely high energy scale of the magnetic cross section of Fe and Ni (see the D values in Table I), it is not possible to map out the entire scattering function $S(Q,\omega)$. On the other hand, some of the $3d$ metallic ferromagnets, such as Pd_2MnSn, can easily be studied by the current thermal neutron scattering technique, utilizing energy transfers of less than 50 meV.

We have selected the intermetallic compound Pd_2MnSn (one of the Heusler family) for this study because of its localized, ferromagnetic nature. The saturated value of the Mn moment is $4.2\mu_B$ which is in good agreement with the value obtained from paramagnetic susceptibility measure-

TABLE I. Cubic ferromagnets. Parameters D, A, and κ_1 are usually given in units of Å^{-1}. In this table A^* and κ_0^* are expressed in units of reduced wave number ζ of the inverse plane distance d^*. Note a narrow range of κ_0^*, in contrast to a very large variation of A^*. d^* corresponds to [110] for Fe and [111] for other ferromagnets. $E=Dq^2$, $\Gamma=Aq^{2.5}$ at T_c, and $\kappa_1^*=\kappa_0^*(T-T_c/T_c)^{0.7}$.

	Ni	Fe	Pd_2MnSn	EuO
T_c (K)	631	1021	190	69
D at $0.8T_c$ (meV Å^2)	330	175	70	7.4
A (meV Å$^{2.5}$)	350	140	60	3.5
$A^*(\zeta)$	5900	2400	230	23
$\kappa_0^*(\zeta)$	0.20	0.34	0.22	0.30
Lattice constant a (Å)	3.5	2.9	6.4	5.2
d^* (Å^{-1})	3.1	3.1	1.7	2.1

ments. Mn forms a face-centered-cubic lattice such as Ni. The pertinent parameters are given in Table I. An extensive study of the spin-wave dispersion relation was already carried out by Noda and Ishikawa.[8] They analyzed the magnon dispersion relation by using a Heisenberg Hamiltonian with long-range magnetic interactions up to the sixth-nearest neighbor. The aim of this current study on Pd_2MnSn is to characterize the paramagnetic scattering from this localized metallic ferromagnet and compare the results with two other representative cubic ferromagnets, insulating EuO and itinerant Ni.

The simplest form of the scattering function is

$$S(Q,\omega)=2kT\chi(0)\frac{\kappa_1^2}{\kappa_1^2+q^2}\frac{1}{\pi}\frac{\Gamma}{\Gamma^2+\omega^2}, \quad (1)$$

where $\chi(0)$ is the uniform susceptibility and κ_1 the inverse correlation length. The linewidth has the form $\Gamma=Aq^{2.5}$ at T_c and changes over to $\Gamma=\Lambda(T)q^2$ in the hydrodynamic limit[9] at higher temperatures. Equation (1) is of course an approximation which is strictly valid only for the small-q, small-ω limit near T_c. At higher ω, we should add the detailed balance factor $\omega/kT(1-e^{(-\omega/kT)})^{-1}$. Moreover, the Lorentzian form in both ω and q must also be modified. We are using Eq. (1) as the simplest starting point to approximate the observed cross section near and above T_c. Figure 1 illustrates the intensity contours calculated with appropriate parameters for Pd_2MnSn using Eq. (1) (detailed balance included). These contours possess the behavior that constant-E scans show definite peaks, even though constant-Q scans are Lorentzians centered around $\Delta E=0$. Therefore, the constant-energy peaks are not necessarily signifying propagating spin waves. We will return to this point after we describe our results which were carried out using the orthodox technique of constant-Q scans.

We will also compare our results with recent neutron scattering studies on Pd_2MnSn by Ziebeck *et al.*[10] Our experimental results are, in many important aspects, in agreement with those of Ziebeck *et al.* On the other hand, our experiments were carried out in an entirely different perspective, resulting in a different physical picture of the paramagnetic scattering.

II. EXPERIMENTAL DETAILS

The single crystal used in the present study was grown at Tohoku University using the Bridgeman method. It has a volume of approximately 3 cm^3 and was mounted in the (hhl) zone. We have decided to concentrate our $S(Q,\omega)$ scan along the [111] direction, where previous studies on a single crystal of EuO were carried out.[11] We first identified the Curie temperature from the depolarization of the polarized neutron beam by the sample. As shown in the inset of Fig. 2, there is a considerable spread of more than 10 K for the gradual depolarization. A similar test on Ni shows almost a discontinuous change at T_c within 1 K. Thus we conclude that a sizable spread of the Curie temperature is present in the crystal, probably due to local inhomogenities of the concentration. We have identified the average value of T_c at 193 ± 3 K from the peak of the critical scattering as shown in Fig. 2.

The neutron scattering measurements were carried out on triple-axis spectrometers at the Brookhaven High-Flux-Beam Reactor. Both polarized and unpolarized beam techniques were combined to obtain an overall picture of the paramagnetic scattering. The polarization analysis[12] of the scattered polarized beam was the essen-

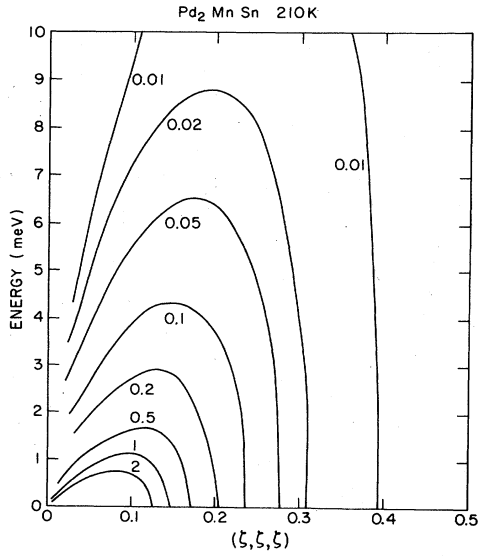

FIG. 1. Contour map for the simple paramagnetic scattering function [Eq. (1)] calculated using parameters given in Table I. Note that a peak is present in constant-E slices but not in constant-Q scans. For $\zeta>0.2$, the contour lines are modified as described in the text.

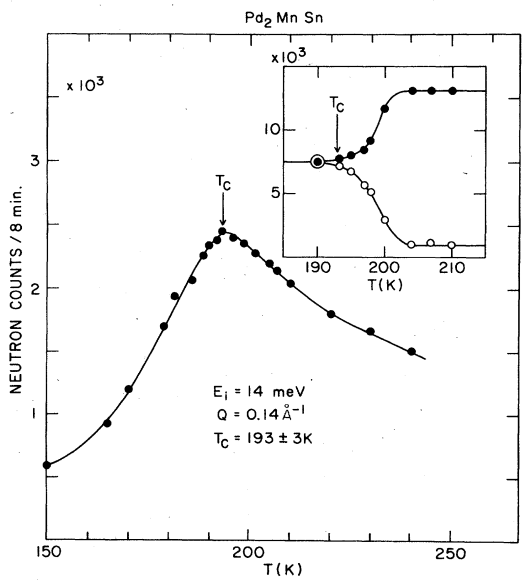

FIG. 2. Determination of the Curie temperature for Pd_2MnSn. A considerable broadening for the depolarization curve is seen in the inset where the solid and open circles correspond to flipper on and off, respectively.

TABLE II. Magnetic σ_M and nuclear σ_N neutron cross sections for the polarization analysis setup. E_f is fixed and flipper is placed after sample. Other notations are nuclear spin incoherent (NSI) and background (BG).

	Flipper on (+ −)	Flipper off (+ +)
Horizontal field	$\sigma_M+\frac{2}{3}\sigma_{\rm NSI}+\sigma_{\rm BG}$	$\sigma_N+0\sigma_M+\frac{1}{3}\sigma_{\rm NSI}+\sigma_{\rm BG}$
Vertical field	$\frac{1}{2}\sigma_M+\frac{2}{3}\sigma_{\rm NSI}+\sigma_{\rm BG}$	$\sigma_N+\frac{1}{2}\sigma_M+\frac{1}{3}\sigma_{\rm NSI}+\sigma_{\rm BG}$

tial ingredient in obtaining the proper picture. Both the monochromator and analyzer are Heusler (111) transmission crystals operating with the final energy E_f fixed. The flipping ratio ranges between 20 and 14 for E_f values between 14 and 30 meV. We have used three different types of scans: (A) polarized-beam data obtained from the difference of horizontal (HF) and vertical (VF) magnetic field data, (B) use of flipper-on data alone, and (C) unpolarized, high- resolution data. The type-(A) scan, which is the most reliable, was first advocated by Moon *et al.*[12] in 1969, but has been put into practical use only recently by Ziebeck, Brown, and their collaborators.[10]

Let us now carefully study Table II. The most uncertain element in neutron experiments is the background (BG), which comes from everything in the beam path excluding the sample. It can also come through the counter shield; thus it is not compensated for by the beam monitor. For example, when E_f is fixed at 30 meV, the counting time for $\Delta E=0$ and $\Delta=30$ meV can easily differ by a factor of 2. This can result in an energy-dependent background which cannot be reliably estimated. Thus when the magnetic cross section σ_M is weak, the difference technique is the only reliable one as has been emphasized by Ziebeck and Brown.[13] Note the difference of $\sigma_{\rm HF}-\sigma_{\rm VF}$ with the flipper on gives the identical information to that of $\sigma_{\rm VF}-\sigma_{\rm HF}$ with the flipper off; that is, $\frac{1}{2}\sigma_M$. If σ_M is large compared with $\sigma_{\rm NSI}+\sigma_{\rm BG}$, then the flipper-on data alone is sufficient. Further, when the nuclear cross section σ_N is small, such as the case with small-angle scattering or magnetic cross sections at energies exceeding all phonon energies, then one can take advantage of the high resolution and high intensity of the unpolarized beam setup. In our current experimental setup, both the horizontal and vertical magnetic fields are only 20 Oe, just enough to maintain the neutron polarization. All neutron measurements below T_c automatically become unpolarized. We have performed limited measurements on spin waves below T_c as shown in Fig. 3; these results are in good agreement with the previous magnon dispersion curves reported by Noda and Ishikawa.[8]

The inverse correlation length κ_1^* is measured by the standard double axis configuration with 14-meV E_i. Its temperature dependence above T_c (up to 242 K) follows

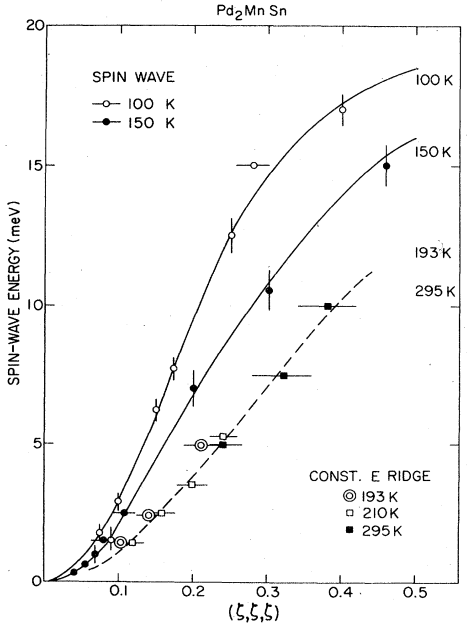

FIG. 3. Spin waves below T_c and constant-E ridges above T_c. These ridges should *not* be confused as spin waves (see text).

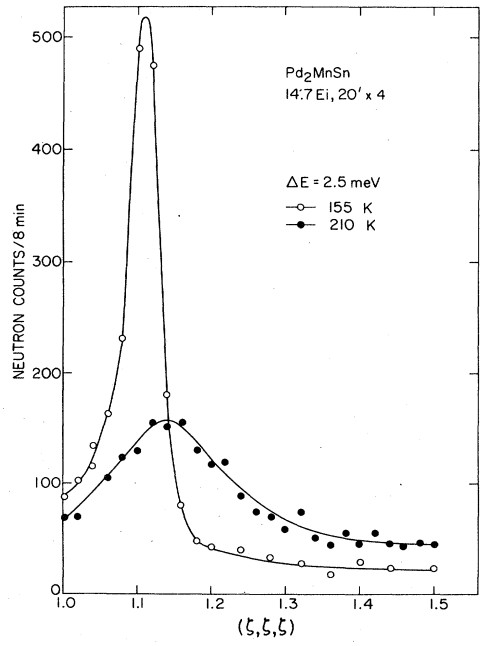

FIG. 4. Typical constant-E scans obtained using unpolarized neutrons. Solid lines are guides to the eye.

the form

$$\kappa_1^* = \kappa_0^* \left[\frac{T - T_c}{T_c} \right]^{\nu} \tag{2}$$

with $\nu = 0.68$ and $\kappa_0^* = 0.22$. Here κ_1^* is expressed in reduced lattice units ζ in the [111] direction. We notice that not only ν but also κ_0^* is quite similar in value with other ferromagnets listed in Table I. At higher temperatures ν changes over to 0.5 and T_c is replaced with T_0. At 295 K, $\kappa_1^* = 0.13$.

III. MAGNETIC SCATTERING ABOVE T_c

Our approach is to establish a simple scattering function using a minimum number of parameters. Figures 4 and 5 show examples of our constant-E and -Q scans taken using different conditions as described in the figure captions. The data at $\zeta = 1.46$ for 210 K is particularly interesting. In contrast to the well-defined magnons observed a finite-energy transfers near the zone boundary between T_c and $1.5T_c$ in EuO, the magnetic response of Pd_2MnSn takes a Lorentzian-like form centered at zero-energy transfer already at T_c for all ζ values up to the [111] zone boundary ($\zeta = 0.5$). We have selected $\zeta = 0.46$ to avoid the higher-order contamination at 0.50. The cross section at 0.46 evolves from a sharp magnon at low temperature to an overdamped form at $T_c = 193$ K and the linewidth Γ becomes somewhat narrower at 295 K. The solid line in Fig. 5 is a calculated cross section with all parameters fixed, as described in detail below. Appropriate resolutions are convoluted into the solid curve.

Figure 6 shows the comparison of the observed linewidths Γ (resolution corrected) with the calculated values at temperatures T_c and 210 K. At T_c the solid circles of the observed linewidth follow with $\Gamma = Aq^{2.5}$ and $A = 60$ meV Å$^{2.5}$ (see Table I). At higher temperatures the overall tendency of the ζ dependence of Γ appears to be approximated by the Résibois-Piette function,[9] though there are certain deviations. This function Ω,

$$\Gamma = Aq^{2.5}\Omega(\kappa_1/q) , \tag{3}$$

passes through unity at $\kappa_1/q = 6$ as q increases. All the data shown in Fig. 6 belong in the range where $\kappa_1/q < 6$. Therefore, the high-temperature data must be below the

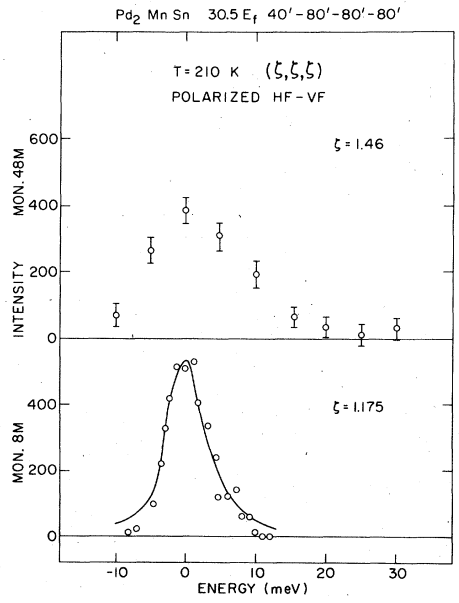

FIG. 5. Examples of magnetic intensity data obtained from the difference of horizontal (HF) and vertical (VF) magnetic field data. The solid line for $\zeta = 1.175$ is the calculated cross section convoluted with the resolution function (see text). Monitor counts of 8 million correspond to approximately 8 min of counting time. The collimations of the triple-axis setup are given at the top.

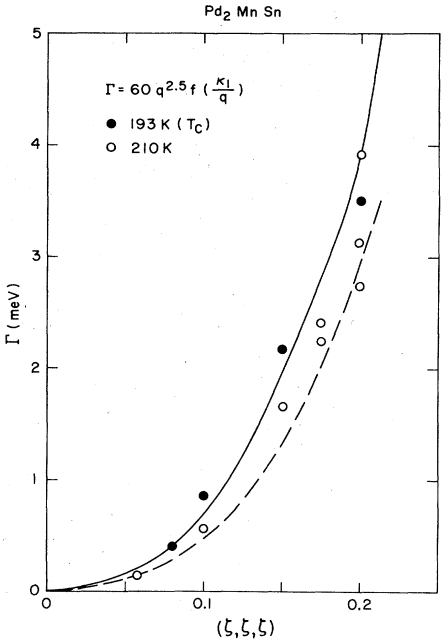

FIG. 6. Comparison of observed and calculated linewidths. The dashed line includes the Résibois-Piette scaling function.

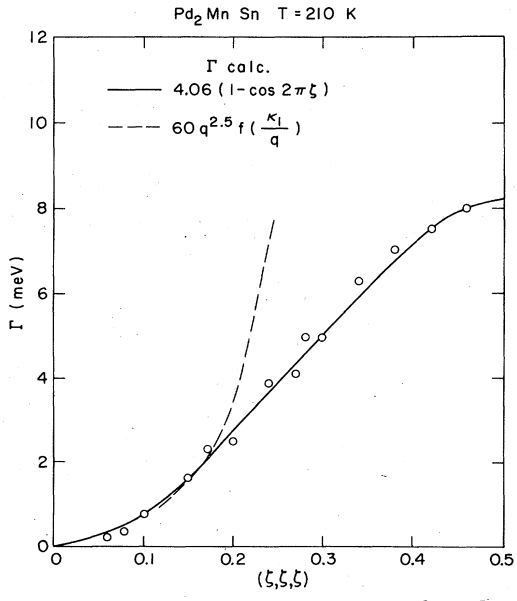

FIG. 7. Linewidth Γ for the entire zone of [111]. The two calculated curves are explained in the text.

$Aq^{2.5}$ lines, even though the initial slope Λ [$\Gamma=\Lambda(T)q^2$] increases with temperature.

Figure 7 lists all the linewidth data taken up to the zone boundary. We immediately noticed that $\Gamma(\zeta)$ resembles the spin-wave energy $E(\zeta)$ at low temperature, namely $1-\cos(2\pi\zeta)$. This is the form valid for ferromagnets with nearest-neighbor interactions only. However, in Pd_2MnSn it is a good approximation for the [111] symmetry direction. The linewidth $\Gamma(\zeta)$ can be expressed as

$$\Gamma(\zeta)=\Lambda_1^*[1-\cos(2\pi\zeta)] \tag{4}$$

with $\Lambda_1^*=4.06$ meV at $T=210$ K. At small ζ, $\Gamma(\zeta)\cong\Lambda_1^*\frac{1}{2}(2\pi\zeta)^2$ (it is more conventional to use $\Gamma=\Lambda_1 q^2$ at small q, with Λ_1 given in units of meV Å^2). This equation is of course an approximation, but it offers a very convenient way to parametrize the scattering function. In spirit, we are approximating the Résibois-Piette function not by the initial slope $\Lambda(T)q^2$ but by $\Lambda_1^*q^2$.

Figure 8 shows the energy integrated paramagnetic scattering defined as follows:

$$M^2(Q)=12\int_0^\infty S(Q,\omega)d\omega\frac{1}{f^2(Q)}\ . \tag{5}$$

These values have been temporarily placed on an absolute intensity scale using the following equation:

$$M^2(Q)=12kT\chi(0)\frac{\kappa_1^2}{\kappa_1^2+q^2}\propto S(S+1)\frac{\kappa_1^2}{\kappa_1^2+q^2} \tag{6}$$

with the known value of the static susceptibility $\chi(0)$ at $T=210$ K. This is shown by the solid line in Fig. 8. Since the significant cross section lies below kT in energy, the high-temperature expression given by Eq. (6) is justified. Deviations of the measured data from this line begin around $\zeta=0.2$. Now we try the same simple modification replacing q^2 by $1-\cos(2\pi\zeta)$. Agreement is improved but not to the level of the linewidth analysis, $\Lambda(\zeta)$. We conclude that the simple scattering function, when appropriately modified, describes the entire range of Q,ω. We have used only two parameters, κ_0^* and Λ_1^*, the latter being closely related to A.

IV. DISCUSSION

We have just demonstrated that the simple paramagnetic scattering function $S(Q,\omega)$ can explain the entire neutron scattering cross section reasonably well. It goes continuously, for the small-ω, small-q limit, to the critical scattering formula. For larger q, it transforms via a simple $1-\cos(2\pi\zeta)$ modification. Thus, the paramagnetic correlations in the localized ferromagnet Pd_2MnSn can be described adequately by the temperature-dependent, "normal" short-range order given by κ_1. One of the most important results of the current study is the disappearance of spin waves near the zone boundary at T_c. As we already remarked, this is in contrast to the case of EuO reported by Mook.[11] In a recent study of Pd_2MnSn, Ziebeck *et al.*[10] briefly reported the inelastic scattering at T_c along the principal directions and stated that above 200 K collective excitations cease to exist. Our results are in complete agreement with those of Ziebeck *et al.*[10] in this respect.

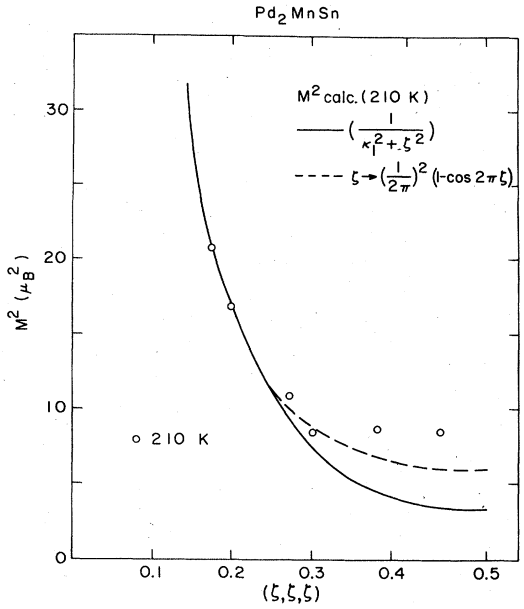

FIG. 8. Magnetic intensity $M^2(Q)$ obtained by the energy integration of $S(Q,\omega)$. The two model calculations are explained in the text using $M^2(0)=325\mu_B^2$ and $\kappa_1=0.08$ Å^{-1} at $T=210$ K.

The major result of the study by Ziebeck *et al.*[10] is the complete paramagnetic scattering of Pd_2MnSn at $T=4T_c$, signified by a constant $M^2(Q)$, after removal of the magnetic form factor. Further polarized-beam studies on Pd_2MnSn for temperatures up to $4T_c$ are currently underway.[14]

Let us now compare the current results with those of Ni and Fe. At T_c the scattering function takes a universal form:

$$S(Q,\omega)\propto\frac{T_c}{A}\kappa_0\frac{q^{0.5}}{q^5+(\omega/A)^2}\ , \tag{7}$$

once we scale the energy by the diffusion constant A. Since the data for Fe and Ni are given[6,7] in the form of constant-E scans, we may compare these scans to the constant-E scan of Pd_2MnSn at $\Delta E=2.5$ meV for 210 K. This temperature is slightly higher than $T_c=193$ K, but the data at T_c is very similar. With use of Table I, this energy transfer scales to 23 meV for Fe and 70 meV for Ni; almost identical peaks were reported around $\zeta=0.14$ for both Fe and Ni in respective constant-E scans.[6,7]

At the beginning of this study we have carried out extensive constant-E scans as shown in Fig. 9. This was following the previous studies on Fe and Ni; we also wanted to demonstrate that these constant-E peaks have nothing to do with a spin-wave picture above T_c. They are simply special slices of the paramagnetic scattering function $S(Q,\omega)$. The peaks of constant-E scans do form a dispersionlike curve, as shown in Fig. 3, and are essentially temperature independent.

During the course of our current investigations we have carefully studied all aspects of $S(Q,\omega)$ in reference to the constant-E scans. This was discussed by Böni *et al.*[15] and

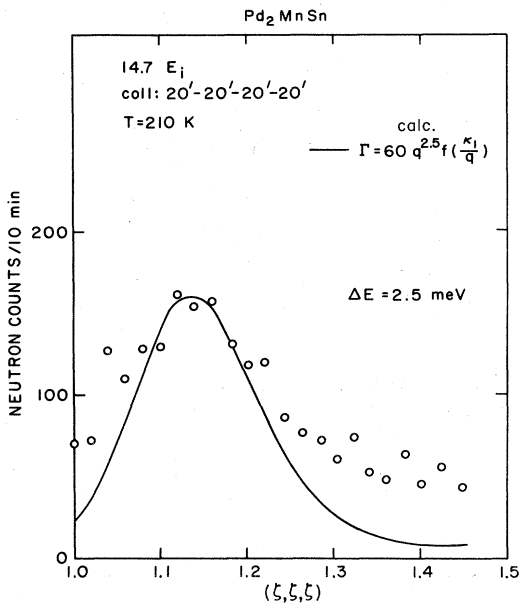

FIG. 9. Constant-E scan at 2.5 meV obtained using unpolarized neutrons. Solid line results from the model calculation described in the text.

demonstrated for Fe by Wicksted *et al.*[16] Therefore, we will not repeat these details here except to remark that the constant-E scans are very sensitive to unimportant details of the scattering function and are not useful in characterizing $S(Q,\omega)$. We do emphasize, however, that Pd_2MnSn gives us the opportunity to study the entire scattering function because of its low-energy scale.[17] It is still puzzling as to why constant-E peaks resemble the magnon dispersion curve. We know that many conditions must be satisfied; $Aq^{2+\delta}$ at T_c, an appropriate D/A ratio, and above all the validity of the simple scattering function $S(Q,\omega)$ at larger q, ω, and T. In particular, if the linewidth Γ above T_c follows the Résibois-Piette function, then a rapid shift of the constant-E profiles is expected. However, these ridges remain temperature independent. It is unlikely that these are all accidental; there must be underlying, simple physical picture which we do not yet comprehend.

Finally, we now address the question which originally motivated this study. What are the differences, in their spin correlations above T_c, between the localized Pd_2MnSn and itinerant Ni? We do not reach the simple conclusions obtained by Ziebeck and Brown: strong temperature-independent correlation for Ni (Ref. 18) and almost no correlation for Pd_2MnSn (Ref. 10). We needed only two parameters to describe the scattering: the diffusion constant A at T_c and the temperature-dependent inverse correlation length

$$\kappa_1^*(T)=\kappa_0^*\left[\frac{T-T_c}{T_c}\right]^{\nu}.$$

We note that κ_0^* is almost identical in value between Ni and Pd_2MnSn in units of respective nearest-neighbor distances d [111] (Table I). We have already demonstrated that the scattering function is identical at T_c, when scaled by A. At present we believe the relevant characteristic parameters are T_c and A; in particular, their ratio. We show A in Table I in units of ζ (denoted by A^*). The ratio of A^*/T_c is 10 for Ni and is 1 for Pd_2MnSn. We tend to compare the results of Ni and Pd_2MnSn in units of T_c. It might be more appropriate to use the temperature scale based on A^*. These are the basic questions we have to resolve before we reach the overall understanding of ferromagnetism in $3d$ metals.[17]

ACKNOWLEDGMENTS

We would like to thank P. Böni, B. H. Grier, O. Steinsvoll, and C. Majkrzak for many stimulating discussions. This work was carried out as a part of the U.S.-Japan collaboration on neutron scattering. Work at Brookhaven supported by the Division of Materials Sciences, U.S. Department of Energy under Contract No. DE-AC02-76CH00016.

[1]See, for example, the recent review article by T. Moriya, J. Magn. Magn. Mater. **31-34**, 10 (1983).
[2]O. Steinsvoll, C. F. Majkrzak, G. Shirane, and J. Wicksted, Phys. Rev. Lett. **51**, 300 (1983); Phys. Rev. B **30**, 2377 (1984).
[3]Y. J. Uemura, G. Shirane, O. Steinsvoll, and J. Wicksted, Phys. Rev. Lett. **51**, 2322 (1983).
[4]J. P. Wicksted, G. Shirane, and O. Steinsvoll, Phys. Rev. B **29**, 488 (1984).
[5]G. Shirane, O. Steinsvoll, Y. J. Uemura, and J. Wicksted, J. Appl. Phys. **55**, 1887 (1984).
[6]J. W. Lynn, Phys. Rev. B **11**, 2624 (1975).
[7]J. W. Lynn and H. A. Mook, Phys. Rev. B **23**, 198 (1981).
[8]Y. Noda and Y. Ishikawa, J. Phys. Soc. Jpn. **40**, 699 (1976).
[9]P. Résibois and C. Piette, Phys. Rev. Lett. **24**, 514 (1970).
[10]K. R. A. Ziebeck, P. J. Webster, P. J. Brown, and J. A. C. Bland, J. Magn. Magn. Mater. **24**, 258 (1981).
[11]H. A. Mook, Phys. Rev. Lett. **46**, 508 (1981).
[12]R. M. Moon, T. Riste, and W. C. Koehler, Phys. Rev. **181**, 920 (1969).
[13]K. R. A. Ziebeck and P. J. Brown, J. Phys. F **10**, 2015 (1980).
[14]M. Kohgi and H. Yoshizawa (private communication).
[15]P. Böni, G. Shirane, and J. P. Wicksted (unpublished).
[16]J. P. Wicksted, P. Böni, and G. Shirane, Phys. Rev. B **30**, 3655 (1984).
[17]See also Y. J. Uemura, in Proceedings of the Conference on High Energy Excitations in Condenced Matter, Los Alamos, 1984 (unpublished).
[18]P. J. Brown, H. Capellmann, J. Deportes, D. Givord, and K. R. A. Ziebeck, J. Magn. Magn. Mater. **31-34**, 295 (1983).